

Intrinsic electron mobility in narrow $\text{Ga}_{0.47}\text{In}_{0.53}\text{As}$ quantum wells

Sanghamitra Mukhopadhyay and B. R. Nag

Calcutta University, Sisir Mitra Bhavan, 92, Acharya Prafulla Chandra Road, Calcutta 700 009, India

(Received 1 February 1993; revised manuscript received 9 September 1993)

Electron mobility in $\text{Ga}_{0.47}\text{In}_{0.53}\text{As}$ quantum wells is calculated for well widths between 2 and 10 nm and for the temperatures of 4.2, 77, and 300 K. Effects of the finite barrier height, energy-band nonparabolicity, mode confinement, electron screening, and degeneracy have been taken into account. The calculated values are found to be close to the experimental results for a well width of 10 nm. Effects of the composition of the barrier layer are also discussed.

I. INTRODUCTION

$\text{Ga}_{0.47}\text{In}_{0.53}\text{As}$ is being increasingly used in various quantum-well electron devices, since its superior transport properties lead to better performance characteristics for the devices. Further, as its energy band gap matches the low loss window of optical fibers it is considered to be the most potent material for quantum-well optoelectronic devices. Modulation-doped structures of $\text{Ga}_{0.47}\text{In}_{0.53}\text{As}/\text{InP}$ have been grown by several techniques and used already to construct high electron mobility transistors¹ and multiple quantum well² lasers.

The quality of the material is often judged by the values of electron mobility in the grown structures. The mobility is determined by the intrinsic scattering processes, i.e., by the alloy and lattice scattering and also by the structural imperfections and impurities. Comparison of the experimental values of mobility with those determined by only the intrinsic scattering processes, therefore, enable one to assess the purity of the structures. Properly calculated theoretical values of intrinsic mobility are required for this purpose.

Experimental structures are grown as single or multiple quantum wells. The multiple wells are, however, separated by thick barrier layers so that the constituent wells may be treated as single wells. The wells have thicknesses down to about 2 nm. The barrier potential in $\text{Ga}_{0.47}\text{In}_{0.53}\text{As}/\text{InP}$ wells is such that for such narrow wells the electron wave function extends significantly into the barrier layers. Also, the subband energy being large, the effect of the energy band nonparabolicity is significant. Further, the character of the phonons, particularly that of polar-optic phonons, is drastically altered. Three different kinds of phonons, the confined phonons, surface phonons, and half-space phonons, are required to be considered. Electron density in the wells is also such that the effects of screening and degeneracy cannot be neglected.

The purpose of this paper is to develop the theory of electron mobility taking into account all the above-mentioned complexities. Theory is then applied to compute the intrinsic electron mobility in $\text{Ga}_{0.47}\text{In}_{0.53}\text{As}$ wells for widths ranging between 2 and 10 nm at temperatures of 4.2, 77, and 300 K.

II. FORMULA FOR THE MOBILITY

Electron mobility is given by

$$\mu = \mathcal{E}^{-2} \vec{\mathcal{E}} \cdot \left[\int \hbar^{-1} (\nabla_{\mathbf{k}} E) f(\mathbf{k}) d\mathbf{k} \right] \left[\int f(\mathbf{k}) d\mathbf{k} \right]^{-1}, \quad (1)$$

where $\vec{\mathcal{E}}$ is the applied electric field, $\hbar^{-1} (\nabla_{\mathbf{k}} E)$ gives the electron velocity corresponding to the kinetic energy E and the pseudomomentum $\hbar\mathbf{k}$, $2\pi\hbar$ is Planck's constant, and \mathbf{k} is the two-dimensional (2D) in-plane wave vector, $f(\mathbf{k})$ is the distribution function of the electrons in the presence of the field, and $d\mathbf{k}$ is an elemental area in the 2D k space.

The distribution function is obtained by solving the Boltzmann transport equation:

$$\begin{aligned} e\hbar^{-1} \vec{\mathcal{E}} \cdot \nabla_{\mathbf{k}} f(\mathbf{k}) = & (A/4\pi^2) \\ & \times \int \{ S(\mathbf{k}, \mathbf{k}') f(\mathbf{k}) [1 - f(\mathbf{k}')] \\ & - S(\mathbf{k}', \mathbf{k}) f(\mathbf{k}') [1 - f(\mathbf{k})] \} d\mathbf{k}', \end{aligned} \quad (2)$$

where A is the sample area, $S(\mathbf{k}, \mathbf{k}')$ is the probability of scattering from the \mathbf{k} state to the \mathbf{k}' state, and $S(\mathbf{k}', \mathbf{k})$ that from the \mathbf{k}' state to the \mathbf{k} state.

Equation (2) is transformed by putting³ (see Appendix A)

$$f(\mathbf{k}) = f_0(E) - (e\hbar/m^*) [\partial f_0(E)/\partial E] \vec{\mathcal{E}} \cdot \mathbf{k} \phi(E), \quad (3)$$

to

$$\begin{aligned} \sum_i S_i(E) \phi(E) - \sum_{+,-} S_{\pm}(E) \phi(E \pm \hbar\omega_l) H(E - \hbar\omega_l) \\ = m^*/m_v(E), \end{aligned} \quad (4)$$

where $f_0(E)$ is the distribution function for the electrons in the absence of the field, m^* is the band-edge effective mass, and $\phi(E)$ is the unknown function giving the perturbation in the distribution function caused by the field; $S_i(E)$ is the difference of the out-scattering and the in-scattering rate for the i th kind of elastic scattering, while for polar optic phonon scattering, $S_i(E)$ is the out-scattering rate, $S_+(E)$ is the in-scattering rate due to optic-phonon absorption, and $S_-(E)$ that due to optic

phonon emission; $H(E - \hbar\omega_l)$ is the Heaviside unit function, $\hbar\omega_l$ is the optic-phonon energy; $m_v(E)$, the so-called velocity effective mass, has been substituted for $\hbar^2 k (\nabla_k E)^{-1}$. The perturbation function $\phi(E)$ may be obtained by solving Eq. (4) with an iteration method.³

The mobility is given in terms of $\phi(E)$ by the following formula:

$$\mu = -(e/m^*) \left[\int m_E(E) [\partial f_0(E)/\partial E] \phi(E) dE \right] \times \left[\int f_0(E) m_v(E) dE \right]^{-1}, \quad (5)$$

where $m_E(E)$ is defined as $\hbar^2 k^2 / 2E$ and is the so-called energy effective mass.

Detailed expressions for the scattering rates are required for obtaining $\phi(E)$. These are discussed in the following section.

III. SCATTERING RATES

Four intrinsic scattering mechanisms are required to be considered. These are alloy scattering, deformation potential acoustic-phonon scattering, piezoelectric scattering, and polar-optic-phonon scattering. We have not, however, included piezoelectric scattering as it contributes significantly only at low temperatures but its contribution is negligible in comparison to that of alloy scattering, the scattering rate for which is almost independent of temperature. Formulas for the scattering rates for the three scattering mechanisms were taken from Refs. 4–7, and are given in Appendix B.

It should be mentioned that the difference in the acoustic properties of the two materials forming the well and the barrier layer is ignored and it is assumed that only the bulk-mode acoustic phonons, characteristic of the well layer, are effective. It will be shown later that the contribution of acoustic phonons is smaller than that of the other two scattering mechanisms and hence this simplification will not introduce any significant error.

Polar-optic-phonon scattering, however, determines the near-room-temperature mobility and its modification by the quantum-well potential cannot be neglected. Bulk polar-optic phonons are modified in quantum wells to surface phonons, confined phonons, and half-space phonons.⁶ Scattering by polar-optic phonons is required to be evaluated by considering this modification.

However, the energy separation between the subband levels in narrow quantum wells is such that only the lowest subband is occupied. The wave function being even for this band, the matrix elements for asymmetric phonon modes are equal to zero. Among the two interface modes, the one whose frequency is close to the barrier layer frequency is required to be included, while that having the frequency of the well-layer phonons may be neglected as its coupling constant is small for narrow wells. The coupling constants may also be taken to be equal to its limiting value for very narrow wells, which compensates partially the effect of neglecting the well-layer surface-mode phonon. The phonons for the well layer may also be assumed to correspond to the GaAs mode, which is known to predominate in the bulk materi-

al.⁸ Expressions for the scattering rates for the three kinds of polar-optic phonons were taken from Ref. 7. These are given in Appendix B after including these simplifications.

The effect of screening is accounted for by multiplying the matrix elements for the various scattering mechanisms by the factor $K_s/K(\omega, q)$; K_s is the static dielectric constant and $K(\omega, q)$ is the dynamic dielectric constant corresponding to the frequency ω and the 2D wave number q of the lattice wave. The expression for $K(\omega, q)$ has been taken from Ref. 9, and is given in Appendix C.

IV. RESULTS

A. Low carrier concentration

We first present the mobilities for the $\text{Ga}_{0.47}\text{In}_{0.53}\text{As}/\text{InP}$ system for small values of the electron concentration. The concentration is such that the equilibrium distribution function $f(E)$ may be taken to be Maxwellian. The factor accounting for the effect of screening is also taken as unity.

Energy levels were calculated by assuming the band offset to be 240 meV.¹⁰ Effects of nonparabolicity were included by using the simplified Kane relation:³

$$\hbar^2 k^2 / 2m_i^* = (E - V_i) [1 + \alpha_i (E - V_i)], \quad (6)$$

where $\alpha_i = (1/E_{gi})(1 - m_i^*/m_0)^2$, E_{gi} is the energy band gap, V_i is the band-edge energy, m_i^* is the band-edge mass, and m_0 is the free-electron mass. The same relation was assumed to apply for both the conduction band in the well layer ($i=W$) and the forbidden band in the barrier layer ($i=B$). Values of the physical constants are given in Appendix D.

We first present in Fig. 1 the computed values of room-temperature $m_v(E)$ and $m_E(E)$ for the first sub-

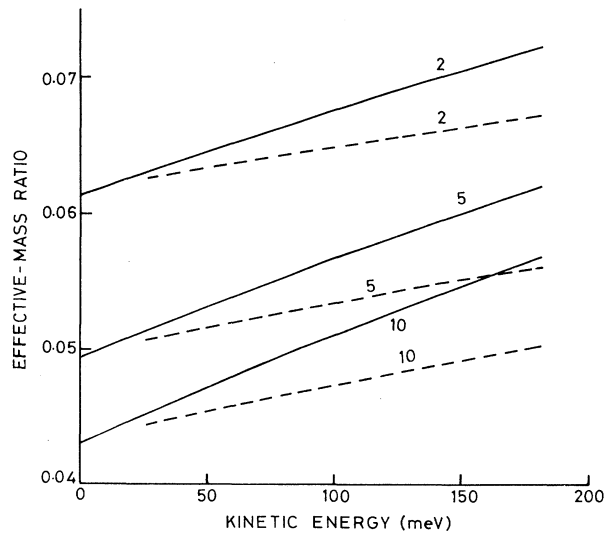


FIG. 1. Velocity and energy effective-mass ratio in wells of different widths. The solid lines are for velocity effective mass and the dashed lines are for energy effective mass.

band, including the effect of the extension of the wave function into the barrier layer and also of the energy-band nonparabolicity. As the electron spends part of the time in the barrier layer due to the extension of the wave function, the effective mass is partly determined by its value in the well material and partly by its value in the barrier material. The barrier material effective mass being larger, the effective value is larger than the well-material mass and the increase is higher for narrower wells due to larger penetration. The effective mass is increased also by the energy-band nonparabolicity with increase in the energy. The two effects add up to cause an increase of the effective mass with the narrowing of the wells. It is seen that the values for small kinetic energies are altered by factors as large as 1.58 for 2-nm-wide wells. Alterations in this value also cannot be considered negligible for larger widths.

The effective mass increases for all wells with increase in the kinetic energy. This increase is caused mainly by the energy-band nonparabolicity. The increase is therefore larger for wider wells as the electron is more confined in the well and the well-material nonparabolicity, which has a larger value, determines the increase. For narrow wells, on the other hand, the penetration being significant, the increase in the effective mass with increase in the kinetic energy is determined partly by the barrier layer nonparabolicity, and as it is smaller, the increase is comparatively smaller.

The form factor¹¹ for the acoustic-phonon scattering is illustrated in Fig. 2. The value is reduced for narrow wells with finite barrier height by large factors. This reduction in the value of the form factor reduces proportionally the scattering rates of scattering mechanisms, the matrix elements for which are independent of q , e.g., deformation potential acoustic-phonon scattering. The

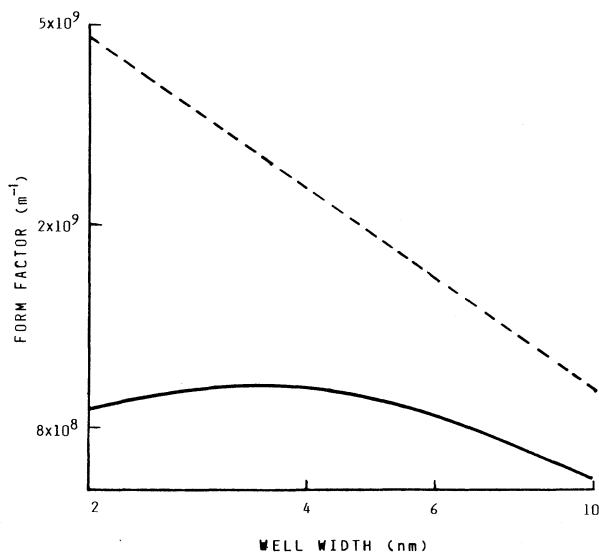


FIG. 2. The form factor for deformation potential acoustic-phonon scattering in wells of different widths. The dashed line is for wells with infinite barrier height and the solid line is for wells with finite barrier height.

effect is, however, less significant for the scattering mechanisms such as polar-optic-phonon scattering, the matrix element for which contains the wave number q_T , as q_T^{-n} , since the form factor is nearly unity for small values of q_z .

Computed values of the mobility for different well widths and different temperatures are shown in Fig. 3 with dashed lines. It is seen that the mobility lies between 0.8 and 1 m^2/Vs at 300 K as the well width is varied between 10 and 2 nm. On the other hand, at 4.2 and 77 K it decreases with decrease in the well width down to about 4nm; then it increases slowly as the width is further decreased.

We have shown the individual contributions of the three intrinsic scattering mechanisms in Fig. 4. It is seen that the mobility is determined fully at 4.2 K by the alloy scattering. At 77 K also, its contribution is about 88%. Lattice scattering is, however, important near room temperature, but the contribution of the acoustic-phonon scattering is less than 10% while that of polar-optic-phonon scattering is more than 60%.

Acceptable standard values of the intrinsic mobility require accurate knowledge of the coupling constants for the scattering mechanisms. Our study indicates that the contribution of the acoustic-phonon scattering being small at all temperatures, error in the value of the deformation potential constant will not be important. We need, however, accurate values of the dielectric constants, the static and also the high-frequency constants, and of the alloy potential. The effect of the uncertainty in the values of the dielectric constants may be considered negligible although these were obtained by inter-

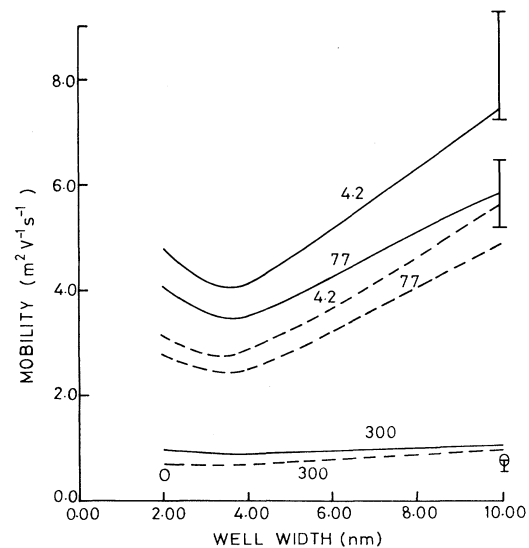


FIG. 3. Electron mobility in $\text{InP}/\text{Ga}_{0.47}\text{In}_{0.53}\text{As}$ wells of different widths. The dashed lines are for samples with low carrier density. The solid lines are for a carrier density of $0.97 \times 10^{12} \text{ m}^{-2}$. Numbers on the curves give the values of lattice temperature. The bars give the range of experimental values for a 10-nm-wide well. Values for $\text{Al}_{0.48}\text{In}_{0.52}\text{As}/\text{Ga}_{0.47}\text{In}_{0.53}\text{As}$ wells are shown by open circles.

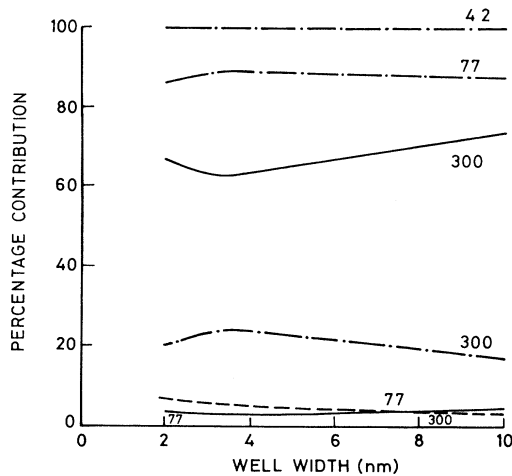


FIG. 4. Percentage contribution of different scattering mechanisms to mobility. The solid lines are for polar-optic-phonon scattering, the dashed lines are for deformation potential acoustic-phonon scattering, and the dot-dashed lines are for alloy scattering. The numbers on the curves give values of lattice temperature.

polation between the values for the constituent components.¹² The coupling constant for the polar optic phonons is 0.0136 for GaAs and 0.0158 for InAs.³ As these values are accurately known from experiments and as the values are close to each other, the interpolated values for $\text{Ga}_{0.47}\text{In}_{0.53}\text{As}$ is also expected to be fairly accurate.

The uncertainty in the computed values of the mobility arises mainly from the value of the alloy scattering potential. The coupling constant for the alloy scattering involves the alloy potential E_{all} , and r_0 , which gives the extent of the potential. But values between 0.42 and 1.1 eV are reported for E_{all} in the literature. The value of r_0 has been taken to be 8.4643 Å, but it is uncertain and may be variable.¹³ The value of $(E_{\text{all}}r_0^3)$ should, therefore, be considered an empirical constant. Calculated values of the mobility presented in this section indicate that it should be possible to fix the value of this constant by studying the mobility in undoped quantum wells of different widths at liquid-nitrogen for lower temperatures.

B. Large carrier concentration

Electron concentration in samples for which experiments have been done is about $1 \times 10^{12} \text{ cm}^{-2}$. Effects of screening and degeneracy cannot be neglected for such concentrations. We have computed the electron mobility for the experimental¹⁴ electron concentration of $0.972 \times 10^{12} \text{ cm}^{-2}$ by including the screening factor and using for $f_0(E)$ the Fermi-Dirac distribution function.

We first present in Fig. 5 the form factor for screening for two extreme well widths and the screening factor (both static and dynamic) for a well width of 2 nm. It is seen that the form factor is nearly independent of the well width for widths between 2 and 10 nm and decreases sharply with $E_q (= \hbar^2 q^2 / 2m^*)$. Values of E_q range between 0 and $4E_F$ (E_F is the Fermi energy) and the form

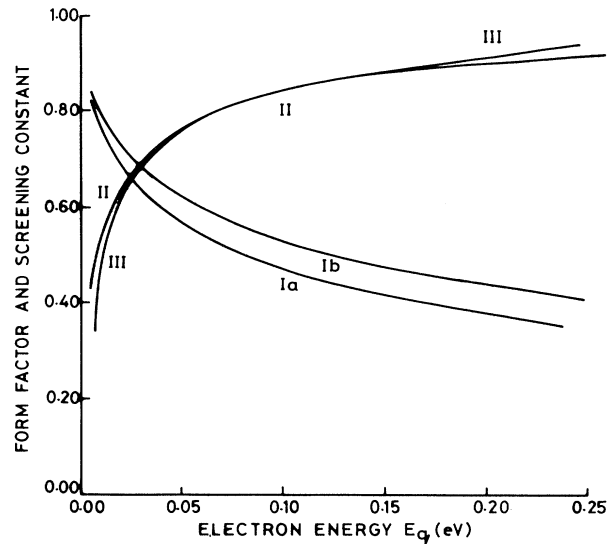


FIG. 5. Form factor and screening constants for the electron energy E_q , corresponding to the phonon wave number q . Ia, form factor for a 10-nm well. Ib, form factor for a 2-nm well. II, static screening constants for a 2-nm well. III, dynamic screening constant for a 2-nm well.

factor for finite barrier height is lowered by about a factor of half in comparison to that for infinite barrier height. This result implies that the screening effect will be reduced by a similar factor in comparison to that estimated earlier by assuming infinite barrier height.

The static ($\omega=0$) screening factor is found to increase from very low values to about unity for the values of E_q ranging between 0 and $4E_F$. In agreement with the expected result discussed above, the finite barrier is found to decrease the effect of screening, i.e., it makes the screening factor closer to unity.

The dynamic screening factor is obtained by assuming that the electron gas remains fully degenerate and the frequency ω of interest is the optic phonon frequency $5.24 \times 10^{13} \text{ rad/sec}$. We find that the curve is very close to that for static screening. There are very small deviations for very low and very high values of E_q . It should be mentioned that screening of polar-optical fields has not been considered earlier.¹⁵ Our calculations indicate that polar fields will be screened by almost the same factor as other scattering fields, apparently because the frequency ω is not high enough to make the static and dynamic screening constants significantly different.

The computed values of mobility including the effects of screening and degeneracy are shown by solid lines in Fig. 3. It is seen that the nature of variation of the mobility with temperature or well width is not significantly altered, but the values are increased by factors of 1.2–1.5.

Available experimental results are also shown in Fig. 3. These values have some variations as shown by the bars. Our computed values, including the effect of screening and degeneracy, fall within the range of experimental values for the lattice temperatures of 77 and 4.2 K. The value is, however, about 20% higher at 300 K. Implication of this discrepancy cannot be assessed at this stage

since only one set of experimental results for the well width of 10 nm is available. Experiments covering a wider range of well widths may clarify the disagreement.

Computations were also done for the electron mobility in $\text{Ga}_{0.47}\text{In}_{0.53}\text{As}$ wells for barriers of $\text{Al}_{0.48}\text{In}_{0.52}\text{As}$, which are also currently used in devices. Values for 300 K, including the effects of screening and degeneracy, are shown for the two extreme well widths. It is seen that the mobility for the $\text{Al}_{0.48}\text{In}_{0.52}\text{As}$ barriers are lower by about 14% for the well width of 10 nm and 48% for the width of 2 nm when the alloy potential is taken to be 0.4 eV in $\text{Al}_{0.48}\text{In}_{0.52}\text{As}$. These results may be understood by considering that the barrier height in the $\text{Al}_{0.48}\text{In}_{0.52}\text{As}/\text{Ga}_{0.47}\text{In}_{0.53}\text{As}$ system is more than double of that in the $\text{InP}/\text{Ga}_{0.47}\text{In}_{0.53}\text{As}$ system. The electron wave function in the latter system, therefore, extends more into the barrier and also since the alloy scattering is absent in the InP barrier layer, the mobility is further increased and the overall mobility is increased as a result of the wave-function extension. On the other hand, in the $\text{Al}_{0.48}\text{In}_{0.52}\text{As}/\text{Ga}_{0.47}\text{In}_{0.53}\text{As}$ system the electron is more confined in the $\text{Ga}_{0.47}\text{In}_{0.53}\text{As}$ layer and even when it extends into the barrier layer, the scattering is not diminished, since the barrier layer is also an alloy material in this system. It may, therefore, be concluded that the electron mobility in the $\text{Ga}_{0.47}\text{In}_{0.53}\text{As}$ wells will be, in general, lower for the $\text{Al}_{0.48}\text{In}_{0.52}\text{As}$ barriers than that for the InP barrier.

V. CONCLUSION

Theory of electron mobility has been presented for narrow quantum wells, including the effects of wave-function penetration into the barrier layers, energy-band nonparabolicity, confinement of polar-optic vibrations, electron screening, and degeneracy of the electron gas. Theory has been applied to compute the electron mobility in $\text{InP}/\text{Ga}_{0.47}\text{In}_{0.53}\text{As}$ quantum wells. Results obtained by using the chosen values of the physical constants are found to agree with the experiment for the lattice temperatures of 4.2 and 77 K but are about 1.2 times higher for 300 K. Electron mobility in $\text{Al}_{0.48}\text{In}_{0.52}\text{As}/\text{Ga}_{0.47}\text{In}_{0.53}\text{As}$ wells are found to be much lower than those in $\text{InP}/\text{Ga}_{0.47}\text{In}_{0.53}\text{As}$ wells.

ACKNOWLEDGMENTS

S.M. acknowledges the University Grants Commission, Government of India, for financial support.

APPENDIX A: REDUCTION OF THE BOLTZMANN TRANSPORT EQUATION

On replacing $f(\mathbf{k})$ in the Boltzmann equation by the assumed expression involving $\phi(E)$, we obtain³

$$(A/4\pi^2) \int [1-f_0(E')][1-f_0(E)]^{-1} [S(\mathbf{k}, \mathbf{k}') \{ \phi(E) - (\mathbf{k}' \cdot \vec{\epsilon} / \mathbf{k} \cdot \vec{\epsilon}) \phi(E') \}] d\mathbf{k}' = m^* / m_v(E), \quad (\text{A1})$$

where E and E' are the energies corresponding to the k and k' state.

The scattering probability $S(\mathbf{k}, \mathbf{k}')$ may be written in general, as

$$S(\mathbf{k}, \mathbf{k}') = (2\pi/\hbar) [A(|\mathbf{k}' - \mathbf{k}|)C]^2 \delta[E' - (E + \Delta V)], \quad (\text{A2})$$

where $A(|\mathbf{k}' - \mathbf{k}|)$ is the part of the matrix element which depends on the phonon wave vector $\mathbf{q} = \mathbf{k}' - \mathbf{k}$ and C is the part which depends on the physical constants of the material. ΔV is the change in energy of the electron due to scattering and $\delta(x)$ is the Dirac δ function.

The first term in the integral of Eq. (A1) corresponds to out-scattering from the \mathbf{k} state to the \mathbf{k}' state. The integration is carried out by using the property of the δ function to obtain

$$\begin{aligned} (A/4\pi^2) \int [1-f_0(E')][1-f_0(E)]^{-1} S(\mathbf{k}, \mathbf{k}') \phi(E) d\mathbf{k}' &= (A/4\pi^2) \int_0^{2\pi} [1-f_0(E')][1-f_0(E)]^{-1} (2\pi/\hbar) C^2 (1/\hbar^2) \\ &\times [A\{(\mathbf{k}'^2 + k^2 - 2kk' \cos\beta)^{1/2}\}]^2 \phi(E) m_v(E) d\beta \\ &= S_{\text{out}}(E) \phi(E), \end{aligned} \quad (\text{A3})$$

where β is the angle between \mathbf{k} and \mathbf{k}' , and $E' = E + \Delta V$, and \mathbf{k} and \mathbf{k}' have the values corresponding to E and $E + \Delta V$.

The second term representing the in-scattering from the \mathbf{k}' to the \mathbf{k} state may be reduced by following the same procedure to $S_{\text{in}}(E) \phi(E + \Delta V)$. It involves, however, the extra term $\mathbf{k}' \cdot \vec{\epsilon} / \mathbf{k} \cdot \vec{\epsilon}$.

APPENDIX B:

FORMULA FOR THE SCATTERING RATES

1. Alloy scattering

Expression for the scattering rate for the alloy scattering⁴ has been taken from Ref. 4. It is given below:

$$S_{\text{all}}(E) = m_v(E) \int_{-\infty}^{\infty} C_{\text{all}}(z_0) |F(z_0)|^4 dz_0,$$

where

$$\begin{aligned} C_{\text{all}}(z_0) &= (1/\hbar^3) [(4\pi/3) E_{\text{all}}(z_0) r_0^3(z_0)]^2 \\ &\times x(z_0) [1 - x(z_0)] N/2. \end{aligned} \quad (\text{B1})$$

E_{all} is the alloy scattering potential, $r_0(z_0)$ is the radius of the sphere over which the alloy potential is assumed to be effective, $x(z_0)[1 - x(z_0)]N/2$ is the concentration of scattering centers, x is the value of the fraction in the material taken in general as $A_x B_{1-x} C$; N is the number of atoms per unit volume of the crystal; $F(z_0)$ is the en-

velope function describing the electron behavior in the well at the location of the scattering center, z_0 .

2. Deformation potential acoustic-phonon scattering

Expression for the acoustic-phonon scattering rate has been taken from Ref. 5. The scattering rate is given by

$$S_{ac}(E) = C_{ac} [m_v^*(E)/m^*] \int_{-\infty}^{\infty} |G(q_z)|^2 dq_z ,$$

where

$$C_{ac} = E_{ac}^2 k_B T m^* / 4\pi\rho s^2 \hbar^3 .$$

$$G(q_z) = \int_{-\infty}^{\infty} F^*(z) F(z) \cos(q_z z) dz , \quad (B2)$$

$$F(z) = H(z - L/2) F_B(z) + H(L/2 - |z|) F_W(z) .$$

E_{ac} is the acoustic-phonon deformation potential constant, ρ is the density of the material, s is the acoustic velocity. $G(q_z)$ is the form factor for electron-phonon interaction corresponding to the z component q_z , of the phonon wave number. $F_W(z)$ and $F_B(z)$ are the envelope functions for the well and the barrier region, respectively, L is the width of the well, k_B is the Boltzmann constant, and T is the lattice temperature.

3. Polar-optic-phonon scattering

There are three kinds of polar phonons: the surface phonons, the confined phonons, and the half-space phonons. Expressions for the out-scattering rates indicated by the subscripts S , C , and H , respectively, for the three modes are given below.

Surface phonons

$$S_s(E) = \sum_{+,-} \alpha_{s\pm} \int_0^{2\pi} [m_v^*(E)/m^*] R_{s\pm} d\theta .$$

where

$$\alpha_{s\pm} = m^* e^2 \omega_{IB} (1/K_{\infty B} - 1/K_{sB}) (8\pi\epsilon_0 \hbar^2)^{-1} \times (n_{0B} \pm \frac{1}{2} + \frac{1}{2}) ,$$

$$R_{s\pm} = |G_s(q)|^2 / (|\mathbf{k}_{\pm} - \mathbf{k}|) ,$$

$$q = |\mathbf{k}_{\pm} - \mathbf{k}| ,$$

$$G_s(q) = \int_{-\infty}^{\infty} F^2(z) f_s(q, z) dz ,$$

$$f_s(q, z) = \begin{cases} \exp[q(z - L/2)] & \text{for } |z| < L/2 , \\ \exp[-q(z - L/2)] & \text{for } z > L/2 , \\ \exp[q(z - L/2)] & \text{for } z < -L/2 . \end{cases} \quad (B3)$$

Confined phonons

$$S_c(E) = \sum_{+,-} \sum_m \alpha_{c\pm} \int_0^{2\pi} [m_v^*(E)/m^*] R_{c\pm} d\theta ,$$

where $m = 1, 3, 5, \dots$,

$$\alpha_{c\pm} = m^* e^2 \omega_{lw} (1/K_{\infty W} - 1/K_{sW}) (2\pi \hbar^2 \epsilon_0 L)^{-1} \times (n_{0W} + \frac{1}{2} \pm \frac{1}{2}) ,$$

$$R_{c\pm} = |G_c(m)|^2 / [q^2 + (m\pi/L)^2] ,$$

$$q = |\mathbf{k}_{\pm} - \mathbf{k}| , \quad (B4)$$

$$G_c(m) = \int_{-L/2}^{L/2} F^2(z) \cos(m\pi/L) z dz .$$

Half-space phonons

$$S_H(E) = \sum_{+,-} \alpha_H \int_0^{2\pi} \int_{q_z > 0}^{\infty} [m_v^*(E)/m^*] R_{H\pm} d\theta dq_z ,$$

where

$$\alpha_{H\pm} = m^* e^2 \omega_{lW} (1/K_{\infty W} - 1/K_{sW}) (2\pi^2 \epsilon_0 \hbar^2)^{-1} \times (n_{0W} + \frac{1}{2} \pm \frac{1}{2}) ,$$

$$R_{H\pm} = |G_H(q_z)|^2 / [|\mathbf{k}_{\pm} - \mathbf{k}|^2 + q_z^2] , \quad (B5)$$

$$G_H(q_z) = \int_{L/2}^{\infty} F^2(z) \sin[q_z(z - L/2)] dz .$$

In the above expressions, \mathbf{k}_{\pm} are the in-plane wave vectors corresponding to the kinetic energies $E \pm \hbar\omega_l$, ω_l is the polar-optic-phonon frequency, θ is the angle between \mathbf{k}_{\pm} and \mathbf{k} , n_{0i} is the occupation number of polar-optic phonons, K_{si} , $K_{\infty i}$ are, respectively, the static and high-frequency dielectric constants, ϵ_0 is the free space permittivity and the subscripts W and B indicate the values, respectively, for the well and the barrier layer of the structure.

These expressions are obtained from the expressions given in Ref. 6 with the simplifying assumptions discussed in the text.

APPENDIX C: FORMULA FOR THE DYNAMIC DIELECTRIC CONSTANT $K(\omega, q)$

The expression for the dynamic dielectric constant $K(\omega, q)$ as obtained from the random-phase approximation may be written for extremely degenerate electron gas as follows:

$$K(\omega, q)/K_s = 1 + (1/q\lambda_{2D}) F(q) \Pi(\omega, q) , \quad (C1)$$

where ω and q are, respectively, the frequency and the wave number of the lattice wave. λ_{2D} is the 2D screening length and

$$1/\lambda_{2D} = (e^2/2K_s\epsilon_0) (\partial N_s / \partial E_F) \approx m^* e^2 / 2\pi K_s \epsilon_0 \hbar^2 . \quad (C2)$$

$F(q)$ is the form factor given by

$$F(q) = \int_{-\infty}^{\infty} F^2(z) \int_{-\infty}^{\infty} F^2(z') \exp(-q|z - z'|) dz' dz . \quad (C3)$$

$\Pi(\omega, q)$ may be expressed as

$$\begin{aligned}
\Pi(q, \omega) &= [1 - K_{sW}(\omega/cq)^2]^{1/2} (\chi_1 - i\chi_2), \\
\chi_1 &= 1 - \sum_{+,-} C_{\pm} [\frac{1}{4}(1 \pm \hbar\omega/E_q)^2 - E_F/E_q]^{1/2}, \\
\chi_2 &= \sum_{+,-} D_{\pm} [(E_F/E_q) - \frac{1}{4}(1 \pm \hbar\omega/E_q)^2]^{1/2}, \\
C_{\pm} &= \text{sgn}(1 \pm \hbar\omega/E_q), \quad D_{\pm} = 0
\end{aligned} \tag{C4}$$

for

$$(1 \pm \hbar\omega/E_q)^2 > 4E_F/E_q,$$

and

$$C_{\pm} = 0, \quad D_{\pm} = 1$$

for

$$(1 \pm \hbar\omega/E_q)^2 < 4E_F/E_q \tag{C4}$$

and

$$E_q = \hbar^2 q^2 / 2m^*, \quad E_F = \hbar^2 k_F^2 / 2m^*, \tag{C5}$$

k_F being the electron wave vector at the Fermi level E_F , c is the velocity of light in free space.

APPENDIX D: VALUES OF THE PHYSICAL CONSTANTS

$$\begin{aligned}
m_W^* &= 0.042m_0 [1 - 2.0 \times 10^{-4}(T/E_{gW})], \\
\alpha_W &= (1/E_{gW}) [1 - (m_W^*/m_0)]^2 \text{ eV}^{-1}, \\
E_{gW} &= 0.813 [1 - 2.0 \times 10^{-4} \times T] \text{ eV}, \\
m_B^* &= 0.079m_0 [1 - 2.9 \times 10^{-4}(T/E_{gB})], \\
\alpha_B &= (1/E_{gB}) [1 - (m_B^*/m_0)]^2 \text{ eV}^{-1}, \\
E_{gB} &= 1.4236 [1 - 2.9 \times 10^{-4} \times T] \text{ eV}.
\end{aligned}$$

Temperature dependence of the constants was introduced by using the temperature coefficient for the band gap and the assumption that the effective mass varies directly as the band gap.

The following values were taken for the other physical constants:

$$\begin{aligned}
\rho_s^2 &= 12.3 \times 10^{10} \text{ n m}^{-2}, \quad E_{\text{all}} = 0.55 \text{ eV}, \\
E_{ac} &= 9.2 \text{ eV}, \quad r_0 = 8.4643 \text{ \AA}, \quad K_{sW} = 13.88, \\
K_{sB} &= 12.38, \quad K_{\infty W} = 11.34, \quad K_{\infty B} = 9.55, \\
\hbar\omega_{lW} &= 34.5 \text{ meV}, \quad \hbar\omega_{lB} = 43.1 \text{ meV}, \\
\epsilon_0 &= 8.85 \times 10^{-12} \text{ F/m}, \quad m_0 = 9.31 \times 10^{-31} \text{ kg}.
\end{aligned}$$

- ¹W. T. Masselink, A. A. Ketterson, J. Klem, W. Kopp, and H. Morkoc, *Electron. Lett.* **21**, 937 (1985).
²W. T. Tsang, *App. Phys. Lett.* **44**, 288 (1984).
³B. R. Nag, *Electron Transport in Compound Semiconductors* (Springer-Verlag, Berlin, 1980), pp. 139 and 60.
⁴Sanghamitra Mukhopadhyay and B. R. Nag, *Appl. Phys. Lett.* **60**, 2897 (1992).
⁵B. R. Nag and Sanghamitra Mukhopadhyay, *J. Phys. Condens. Matter* **3**, 3757 (1991).
⁶N. Mori and T. Ando, *Phys. Rev. B* **40**, 6175 (1989).
⁷B. R. Nag and Sanghamitra Mukhopadhyay, *Jpn. J. App. Phys.* **31**, 3287 (1992).
⁸S. Yamazaki, A. Ushinokawa, and T. Katoda, *J. Appl. Phys.*

- 51**, 3722 (1980).
⁹F. Stern, *Phys. Rev. Lett.* **18**, 546 (1967).
¹⁰B. K. Ridley, *J. Phys. C* **15**, 5899 (1982).
¹¹B. R. Nag and Sanghamitra Mukhopadhyay, *Appl. Phys. Lett.* **58**, 1056 (1991).
¹²S. R. Ahmed, B. R. Nag, and M. Deb Roy, *Solid-State Electron.* **28**, 1193 (1985).
¹³J. H. Marsh, *Appl. Phys. Lett.* **41**, 732 (1982).
¹⁴L. L. Taylor, M. J. Kane, and S. J. Bass, *Appl. Phys. Lett.* **51**, 180 (1987).
¹⁵T. Kawamura and S. Das Sarma, *Phys. Rev. B* **45**, 3612 (1992).